ON-BOARD SMALL-SIZE PRINTED MONOPOLE ANTENNA INTEGRATED WITH USB CONNECTOR FOR PENTA-BAND WWAN MOBILE PHONE

Kin-Lu Wong and Chih-Hua Chang
Department of Electrical Engineering National Sun Yat-sen University, Kaohsiung 80424, Taiwan; Corresponding author: wongkl@ema.ee.nsysu.edu.tw

Received 6 February 2010

ABSTRACT: *An on-board small-size printed two-strip monopole antenna integrated with a universal series bus (USB) connector and generating two wide operating bands to cover penta-band wireless wide area network operation in the 824–960/1710–2170 MHz bands is presented. The two strips of the antenna are respectively printed on two small no-ground portions of 15 × 25 and 15 × 15 mm^2 (total size 600 mm^2). In-between the two printed strips, there is a protruded ground of 15 × 10 mm^2 to accommodate a USB connector, which serves as the data port of the mobile phone. Also, easy control of the antenna's two wide lower and upper bands can be achieved by respectively adjusting the longer and shorter strips of the printed monopole antenna. That is, the antenna is easy to fabricate and also easy to fine-tune in practical applications. Details of the proposed antenna are presented and discussed. The radiation characteristics of the antenna, including the specific absorption rate results with the presence of the user's head and hand, are also studied.* © 2010 Wiley Periodicals, Inc. Microwave Opt Technol Lett 52:2523–2527, 2010; View this article online at wileyonlinelibrary.com. DOI 10.1002/mop.25537

Key words: *mobile antennas; handset antennas; printed antennas; WWAN antennas; printed monopole antennas*

1. INTRODUCTION

The printed two-strip monopole antenna has an attractive feature of simple structure and has been applied in the mobile phone for achieving penta-band wireless wide area network operation (WWAN) operation in the GSM850/900/1800/1900/UMTS bands [1–3]. These reported printed monopole antennas for WWAN operation are mainly disposed on the no-ground portion of the system circuit board of the mobile phone; they are especially attractive to be positioned at the bottom of the mobile phone such that decreased specific absorption rate (SAR) results [2–9] can be obtained to easily meet the 1.6 W/kg limit of 1-g tissue [10–12]. However, for such applications, there is usually a conflict between the printed WWAN antenna and the universal series bus (USB) connector [13], which is usually mounted at the bottom of the system circuit board as a data port for the mobile phone. This causes a big design issue for accommodating the printed WWAN antenna in the mobile phone.

To solve the problem and to achieve compact integration of the internal WWAN antenna with the USB connector, we present in the article a promising two-strip printed monopole antenna capable of integration of the USB connector at the bottom of the mobile phone. The two radiating strips of the printed monopole antenna are printed on two separate no-ground portions at the bottom edge of the system circuit board. In-between the two no-ground portions, there is a protruded ground of 15 × 10 mm^2 in size to flush with the bottom edge of the circuit board. The size of the protruded ground is large enough to accommodate a USB connector in the mobile phone. This arrangement provides a promising solution to integrate the internal WWAN printed monopole antenna with the USB connector. Further, the printed monopole antenna can provide two wide lower and upper bands to respectively cover the GSM850/900 operation (824–960 MHz) and the GSM1800/1900/UMTS operation (1710–2170 MHz). With wideband operation obtained, the total size of the two no-ground portions used to accommodate the printed monopole antenna is 600 mm^2 only, which is comparable with those required for the reported traditional printed penta-band WWAN antennas that cannot be integrated with the USB connector [1–3]. In this study, details of the proposed on-board printed monopole antenna are described. Design considerations of the antenna are discussed, and results of the fabricated prototype of the antenna are presented. Radiation characteristics of the antenna and its SAR values when the user's head and hand are present are analyzed.

2. DESIGN CONSIDERATIONS OF PROPOSED ANTENNA

Figure 1(a) shows the geometry of the on-board printed monopole antenna integrated with a USB connector for penta-band WWAN mobile phone, and detailed dimensions of the antenna are given in Figure 1(b). A 0.8-mm thick FR4 substrate of length 115 mm and width 50 mm is used as the system circuit board of the mobile phone in the study. The FR4 substrate is of relative permittivity 4.4 and loss tangent 0.024. On the back side of the FR4 substrate or the circuit board, the main ground and the protruded ground are printed. The main ground has a size of 100 × 50 mm^2, whereas the protruded ground has a size of 15 × 10 mm^2 and its one edge is flushed with the bottom edge of circuit board. A USB connector of size 9 × 7 × 3 mm^3 [13] is mounted on the protruded ground as shown in the figure; the mounted USB connector can be seen more clearly in the photos of the fabricated antenna shown in Figure 2, in which a practical USB connector is mounted on the protruded ground.

The printed monopole antenna is disposed on the two no-ground portions on the two sides of the protruded ground. Notice that the two no-ground portions are of different sizes. The larger one has a size of 15 × 25 mm^2 and is used to accommodate the longer radiating strip (strip 1, section BD) of length 40 mm. To generate a resonant mode at about 900 MHz for the GSM850/900 operation, a chip inductor of inductance L = 22 nH is added at about the front point B of the longer strip. This chip inductor can contribute additional inductance to compensate for the increased capacitance resulting from the decreased length of the radiating strip [2, 3, 14–16]. Hence, with the embedded chip inductor, the longer strip can generate a resonant mode at about 900 MHz with a length of 40 mm only (about 0.12 wavelength only, much less than that required for the quarter-wavelength resonant mode). With the length reduction in achieving the desired resonant mode, wideband operation can also be obtained for the antenna's lower band to cover the desired 824–960 MHz band. More detailed effects of the embedded chip inductor on the printed monopole antenna are presented in Figure 5, which will be discussed in the next section.

On the other hand, the smaller no-ground portion of 15 × 15 mm^2 accommodates the shorter radiating strip (strip 2, section CE) of length 32.5 mm. The shorter strip can generate a resonant mode at about 1900 MHz for the antenna's upper band to cover the desired GSM1800/1900/UMTS operation (1710–2170 MHz). In this case, the length of the shorter strip is about 0.21 wavelength of the frequency at 1900 MHz, which is less than that required for the quarter-wavelength resonant mode owing to the substrate loading effect of the circuit board.

Both the longer and shorter strips have a narrow width of 1.5 mm and are excited through the asymmetric 50-Ω T-microstrip feedline, whose one end (point A) is the feeding point of the antenna. In the experiment, point A is further connected to a short 50-Ω microstrip line printed on the front side of the circuit board, which is then connected to a 50-Ω SMA connector on

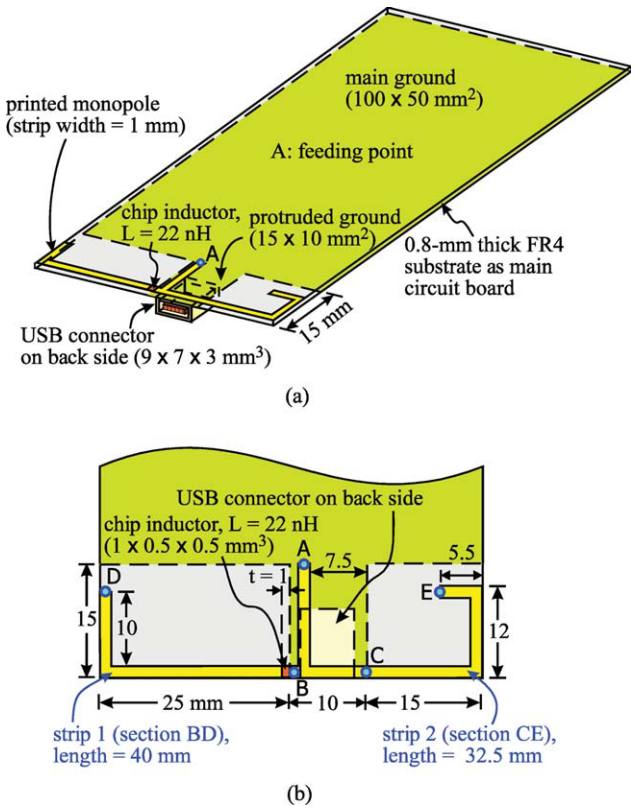

Figure 1 (a) Geometry of the on-board printed monopole antenna integrated with a USB connector for penta-band WWAN mobile phone. (b) Dimensions of the antenna. [Color figure can be viewed in the online issue, which is available at wileyonlinelibrary.com]

the back side of the circuit board (not shown in the figure) to connect to a signal source for testing the antenna in this study. The asymmetric T-microstrip feedline is arranged in the study such that it occupies less board space on the circuit board; hence, more board space can be used for the associated circuit layout on the circuit board.

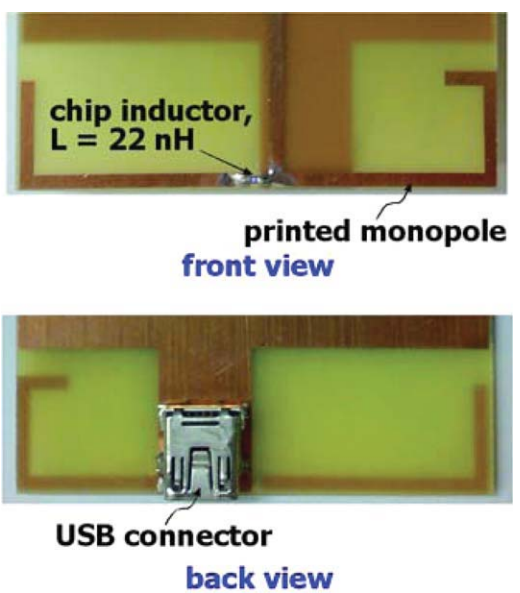

Figure 2 Photos of the fabricated antenna. [Color figure can be viewed in the online issue, which is available at wileyonlinelibrary.com]

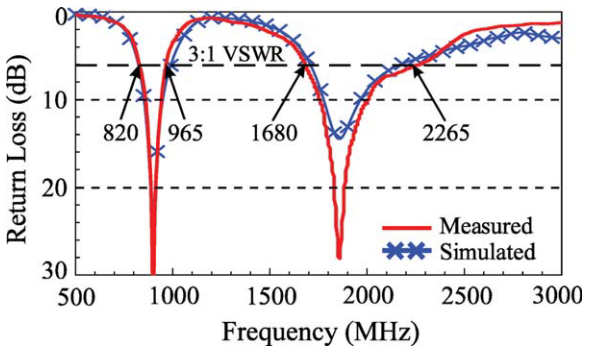

Figure 3 Measured and simulated return loss for the fabricated antenna. [Color figure can be viewed in the online issue, which is available at wileyonlinelibrary.com]

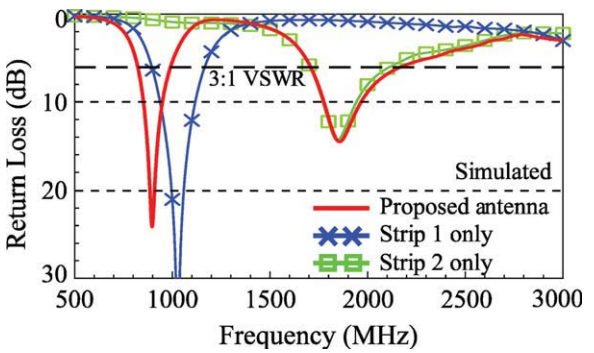

Figure 4 Simulated return loss for the proposed antenna and the two cases with strip 1 only and strip 2 only. [Color figure can be viewed in the online issue, which is available at wileyonlinelibrary.com]

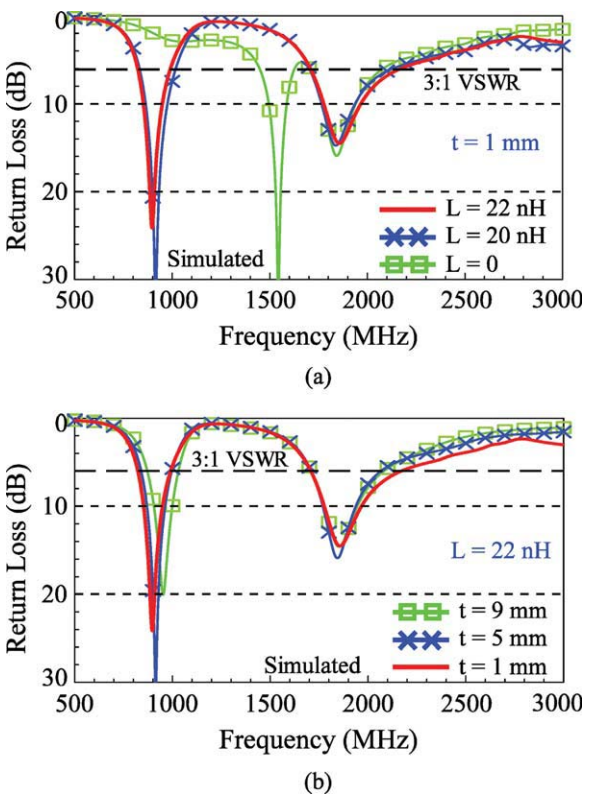

Figure 5 Simulated return loss as a function of (a) the inductance L and (b) the position t of the chip inductor. Other dimensions are the same as given in Figure 1. [Color figure can be viewed in the online issue, which is available at wileyonlinelibrary.com]

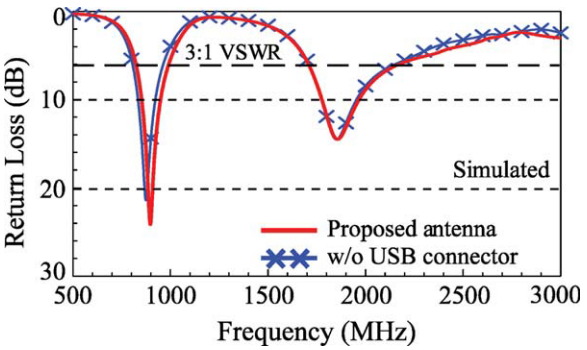

Figure 6 Simulated return loss for the proposed antenna and the case without the USB connector. Other dimensions are the same as given in Figure 1. [Color figure can be viewed in the online issue, which is available at wileyonlinelibrary.com]

3. RESULTS AND DISCUSSION

The proposed antenna was fabricated (see Fig. 2). Results of the measured and simulated return loss for the fabricated antenna are presented in Figure 3. The simulated results are obtained using Ansoft simulation software HFSS version 12 [17]. The measured data agree with the simulated results. Based on the 3:1 VSWR (6-dB return loss), which is widely used as the internal WWAN antenna design specification, the antenna provides two wide operating bands for the desired penta-band WWAN operation in the 824–960/1710–2170 MHz.

The operating principle of the proposed antenna is analyzed. Figure 4 shows the simulated return loss for the proposed antenna and the two cases with strip 1 only and strip 2 only. From the results, it is clearly seen that the antenna's lower and upper bands are contributed by strip 1 (the longer strip) and strip 2 (the shorter strip), respectively. Effects of the embedded chip inductor are studied in Figure 5. Results for different inductances of the chip inductor are presented in Figure 5(a). When the embedded chip inductor is replaced by a simple strip (i.e., $L = 0$), the antenna's lower band occurs at about 1.55 GHz. With increasing inductance, the lower band contributed by the longer strip is quickly shifted to lower frequencies. In the study, with $L = 22$ nH, the lower band can cover the desired 824–960 MHz band. Also notice that the antenna's upper band is almost not affected by the embedded chip inductor. This confirms that the upper band is mainly dominated by the shorter strip in the proposed antenna.

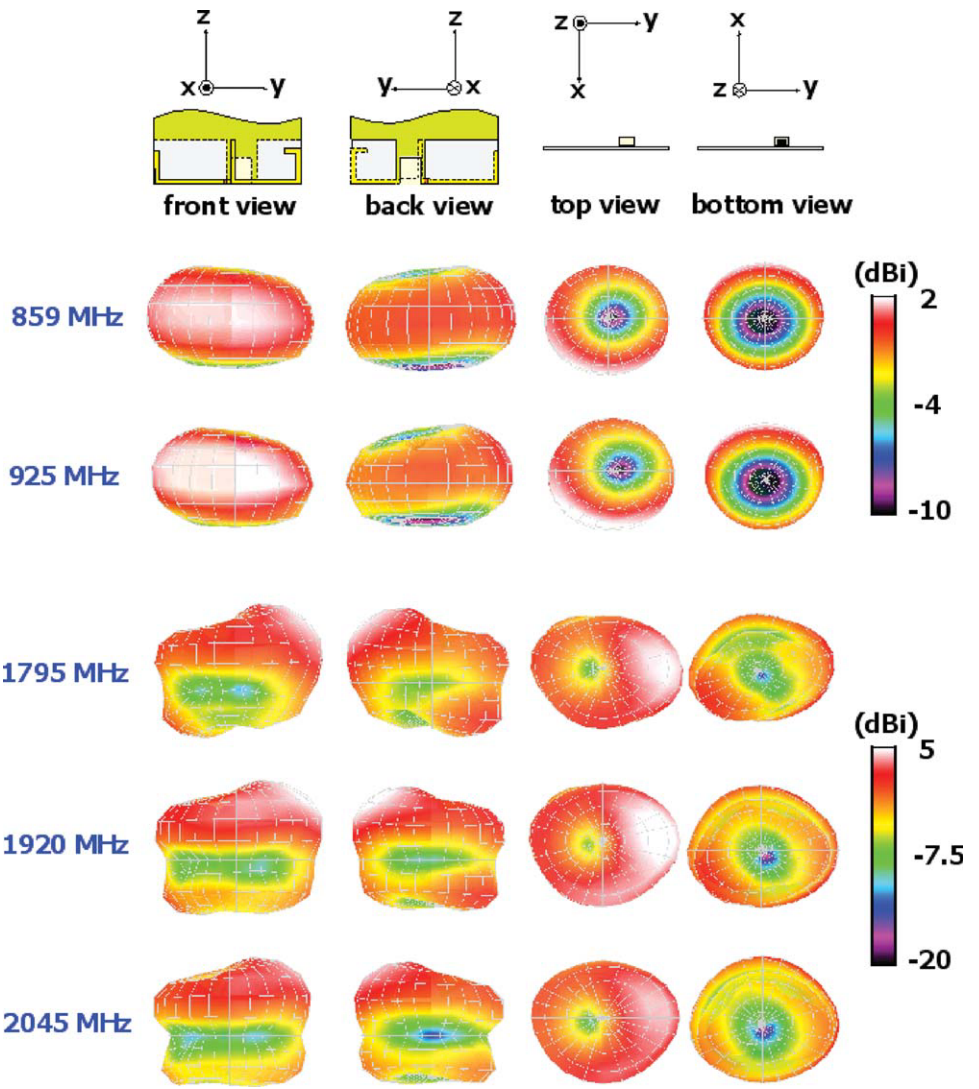

Figure 7 Measured three-dimensional (3D) total power radiation patterns for the proposed antenna. [Color figure can be viewed in the online issue, which is available at wileyonlinelibrary.com]

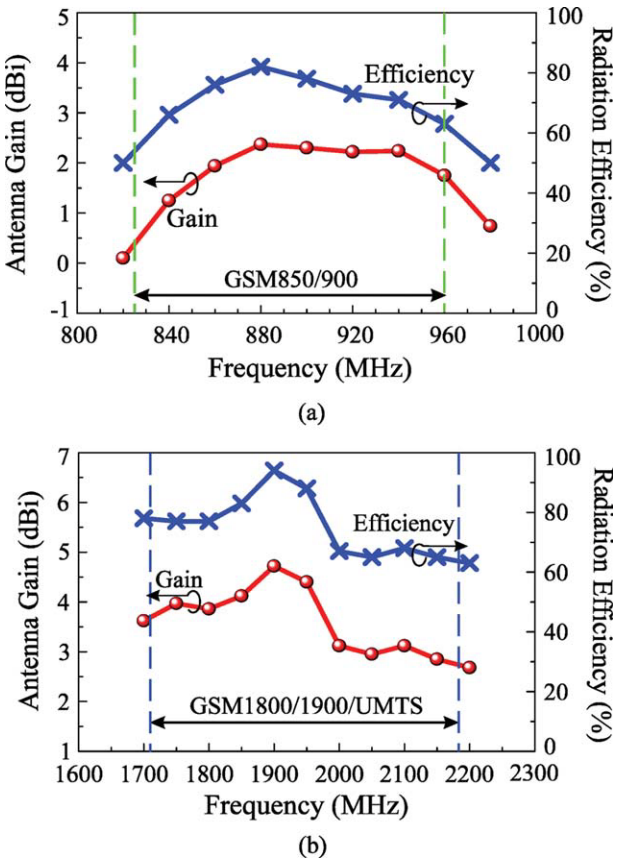

Figure 8 Measured antenna gain and radiation efficiency for the proposed antenna. (a) The lower band for GSM850/900 operation. (b) The upper band for GSM1800/1900/UMTS operation. [Color figure can be viewed in the online issue, which is available at wileyonlinelibrary.com]

Effects of the position t of the chip inductor are analyzed in Figure 5(b), in which the results for the position t varied from 1 to 9 mm are shown. Again, small effects on the antenna's upper band are seen. On the other hand, the lower band is shifted to higher frequencies when the position t increases (i.e., the chip inductor is moved away from the front point B of the longer strip). This behavior is largely related to the excited surface currents on the longer strip; the surface currents are generally stronger on the position closer to the front point of the radiating strip. Hence, the effective inductance contributed by the chip inductor to the input impedance of the antenna will be larger when the chip inductor is embedded closer to the front point of the longer strip. This leads to the differences in shifting the lower band to lower frequencies.

Results of the simulated return loss for the proposed antenna and the case without the USB connector are studied in Figure 6. Notice that the corresponding dimensions of the two antennas studied in Figure 6 are the same. Results indicate that effects of the loaded USB connector on the protruded ground are small. From the results, it can be expected that when other associated electronic components or modules are placed on the protruded ground, their effects on the proposed antenna will also be small. This suggests that with the protruded ground integrated with the proposed antenna in this study, other associated elements in the mobile phone can also be integrated with the proposed antenna. This provides additional alternatives for the proposed antenna in practical mobile phone applications.

Figure 7 shows the measured three-dimensional (3D) total-power radiation patterns for the proposed antenna. Four radiation patterns seen from different directions (front, back, top, and bottom views) at each frequency are shown in the figure. For lower frequencies at 859 and 925 MHz in the antenna's lower band, the radiation patterns looks like those of the traditional half-wavelength dipole antennas. Although for higher frequencies at 1795, 1920, and 2045 MHz in the upper band, more variations or deviations from the dipole-like radiation patterns are seen. However, null radiations in the top and bottom directions are observed, which are similar to those at lower frequencies. The radiation patterns seen at higher frequencies are hence related to those of the higher-order modes of the traditional dipole antennas. This is similar to those observed for the known internal WWAN mobile phone antennas that have been reported [18]. Figure 8 shows the measured antenna gain and radiation efficiency for the proposed antenna. The radiation efficiency for the lower band [Fig. 8(a)] and the upper band [Fig. 8(b)] is about 55–88% and 62–94%, respectively, whereas the antenna gain is about 0.4–2.3 dBi and 2.7–4.6 dBi, respectively.

The SAR results for the proposed antenna are also analyzed. Figure 9 shows the SAR simulation model provided by SEMCAD version 14 [19] and the simulated 1-g SAR values for the proposed antenna. As stated earlier, the antenna is positioned at the bottom of the mobile phone to achieve decreased SAR values. Two cases with the presence of the head phantom and head/hand phantoms are studied. The SAR results are given in the table in the figure. The return loss provided at each testing frequency in the table is the impedance matching level at that frequency. The testing frequencies are the central frequencies of the five operating bands in this study. The grip of the hand phantom on the mobile phone is shown in the figure, and the distance between the palm and the ground plane of the mobile phone is 35 mm, which is reasonable for testing the SAR values with the user's hand presence [12]. The testing

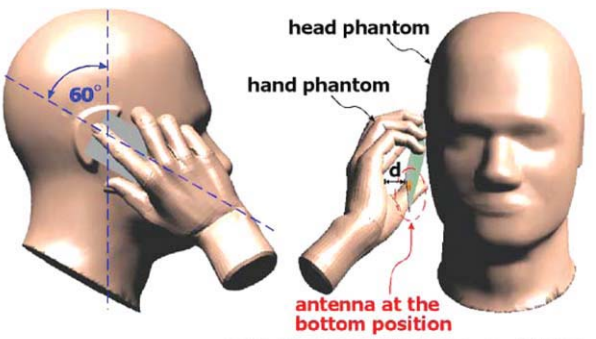

Frequency (MHz)		859	925	1795	1920	2045
1-g SAR (W/kg)	head only	1.30	1.28	0.80	0.76	0.65
	head and hand	1.31	1.30	0.90	0.87	0.76
Return loss (dB)	head only	14.4	11.0	15.4	13.3	8.3
	head and hand	22.1	7.2	32.2	12.3	9.4

Figure 9 SAR simulation model and the simulated 1-g SAR values for the proposed antenna. The return loss given in the table is the impedance matching level at the testing frequency. [Color figure can be viewed in the online issue, which is available at wileyonlinelibrary.com]

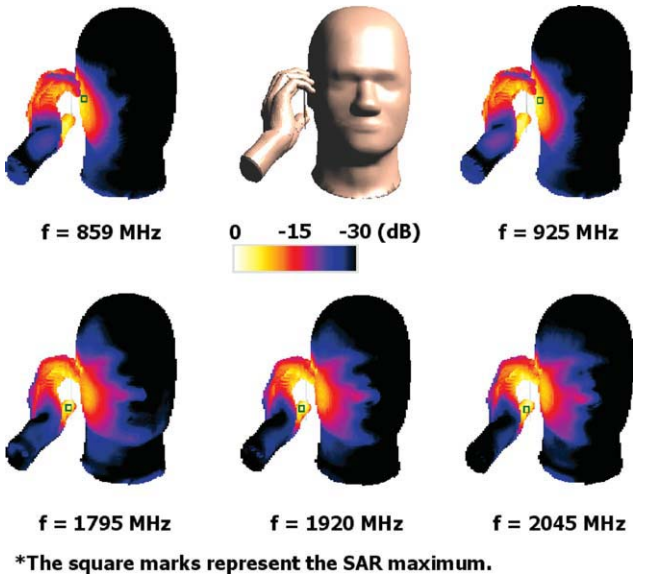

Figure 10 Simulated 1-g SAR distributions on the head and hand phantoms. [Color figure can be viewed in the online issue, which is available at wileyonlinelibrary.com]

power is 24 dBm (2-W continuous input power with a user channel being 1/8 of a time slot) at 859 and 925 MHz for the GSM operation, and 21 dBm at 1795, 1920, and 2045 MHz (1-W continuous input power with a user channel being 1/8 of a time slot at 1795 and 1920 MHz for the GSM operation and 0.125-W continuous input power at 2045 MHz for the UMTS operation). The obtained 1-g SAR values for all the testing frequencies are all well below the 1.6 W/kg limit [10] for both the head only and head/hand cases. It is also interesting to note that the SAR values are higher for the head/hand case than the head only case. This can be seen more clearly from the simulated SAR distributions on the head and hand phantoms shown in Figure 10. For lower frequencies at 859 and 925 MHz in the lower band, the maximum SAR is located on the head phantom. Conversely, for higher frequencies at 1795, 1920, and 2045 MHz in the upper band, the maximum SAR occurs on the head phantom (the thumb of the hand phantom). This causes a larger increase of the SAR value at higher frequencies than at lower frequencies. This behavior needs to be considered when the user's hand is included in the SAR specifications for the internal mobile pone antennas [12].

4. CONCLUSIONS

A small-size two-strip monopole antenna suitable to be printed on the system circuit board of the mobile phone and capable of integration with the USB connector therein has been proposed, fabricated, and tested. The on-board printed antenna is easy to fabricate at low cost and can provide two wide operating bands to respectively cover the GSM850/900 and GSM1800/1900/UMTS operations; that is, penta-band WWAN operation is achieved. Good radiation characteristics for frequencies over the five operating bands have also been observed. The 1-g SAR values for the two cases of head only and head/hand presence are well below the 1.6 W/kg limit, making the proposed antenna very promising for practical mobile phone applications. In addition, owing to its on-board printing characteristic [20–23], the proposed antenna is especially suitable for slim or very slim mobile phone applications.

REFERENCES

1. K.L. Wong and T.W. Kang, GSM850/900/1800/1900/UMTS printed monopole antenna for mobile phone application, Microwave Opt Technol Lett 50 (2008), 3192–3198.
2. T.W. Kang and K.L. Wong, Chip-inductor-embedded small-size printed strip monopole for WWAN operation in the mobile phone, Microwave Opt Technol Lett 51 (2009), 966–971.
3. C.H. Chang and K.L. Wong, Small-size printed monopole with a printed distributed inductor for penta-band WWAN mobile phone application, Microwave Opt Technol Lett 51 (2009), 2903–2908.
4. Y.W. Chi and K.L. Wong, Compact multiband folded loop chip antenna for small-size mobile phone, IEEE Trans Antennas Propag 56 (2008), 3797–3803.
5. C.H. Chang and K.L. Wong, Printed lambda/8-PIFA for penta-band WWAN operation in the mobile phone, IEEE Trans Antennas Propag 57 (2009), 1373–1381.
6. Y.W. Chi and K.L. Wong, Quarter-wavelength printed loop antenna with an internal printed matching circuit for GSM/DCS/PCS/UMTS operation in the mobile phone, IEEE Trans Antennas Propag 57 (2009), 2541–2547.
7. M.R. Hsu and K.L. Wong, Seven-band folded-loop chip antenna for WWAN/WLAN/WiMAX operation in the mobile phone, Microwave Opt Technol Lett 51 (2009), 543–549.
8. K.L. Wong and W.Y. Chen, Small-size printed loop antenna for penta-band thin-profile mobile phone application, Microwave Opt Technol Lett 51 (2009), 1512–1517.
9. W.Y. Chen and K.L. Wong, Small-size coupled-fed shorted T-monopole for internal WWAN antenna in the slim mobile phone, Microwave Opt Technol Lett 52 (2010), 257–262.
10. American National Standards Institute (ANSI), Safety levels with respect to human exposure to radio-frequency electromagnetic field, 3 kHz to 300 GHz, ANSI/IEEE standard C95.1, April 1999.
11. J.C. Lin, Specific absorption rates induced in head tissues by microwave radiation from cell phones, Microwave 40 (2001), 22–25.
12. C.H. Li, E. Ofli, N. Chavannes, and N. Kuster, Effects of hand phantom on mobile phone antenna performance, IEEE Trans Antennas Propag 57 (2009), 2763–2770.
13. http://en.wikipedia.org/wiki/Universal_Serial_Bus, Wikipedia, the free encyclopedia: Universal Serial Bus (USB).
14. T.H. Chang and J.F. Kiang, Meshed antenna reduction by embedding inductors, IEEE Antennas Propag Soc Int Symp USNC/URSI Nat Radio Sci Meet, Washington, DC, USA, Session 78, 2005.
15. J. Thaysen and K.B. Jakobsen, A size reduction technique for mobile phone PIFA antennas using lumped inductors, Microwave J 48 (2005), 114–126.
16. T.W. Kang and K.L. Wong, Very-small-size printed monopole with embedded chip inductor for 2.4/5.2/5.8 GHz WLAN laptop computer antenna, Microwave Opt Technol Lett 51 (2010), 171–177.
17. Ansoft Corporation HFSS; Pittsburgh, PA. Available at: http://www.ansoft.com/products/hf/hfss/.
18. K.L. Wong, Planar Antennas for Wireless Communications, Wiley, New York, 2003.
19. SEMCAD, Schmid & Partner Engineering AG (SPEAG); Available at: http://www.semcad.com.
20. C.I. Lin and K.L. Wong, Printed monopole slot antenna for internal multiband mobile phone antenna, IEEE Trans Antennas Propag 55 (2007), 3690–3697.
21. K.L. Wong and L.C. Lee, Multiband printed monopole slot antenna for WWAN operation in the laptop computer, IEEE Trans Antennas Propag 57 (2009), 324–330.
22. C.T. Lee and K.L. Wong, Uniplanar coupled-fed printed PIFA for WWAN/WLAN operation in the mobile phone, Microwave Opt Technol Lett 51 (2009), 1250–1257.
23. Y.W. Chi and K.L. Wong, Very-small-size printed loop antenna for GSM/DCS/PCS/UMTS operation in the mobile phone, Microwave Opt Technol Lett 51 (2009), 184–192.